TÜBİTAK

Turkish Journal of Chemistry

http://journals.tubitak.gov.tr/chem/

Research Article

Turk J Chem
(2018) 42: 1566 – 1576
© TÜBİTAK
doi:10.3906/kim-1804-67

Exploring inhibition of chemiluminescence mechanisms with fluorescence quenching studies and interaction energy calculations

Zhenbo LIU*, Tangmi YUAN, Yongming LIU, Wenzuo LI, Qingzhong LI, Bo XIAO, Jianbo CHENG
College of Chemistry and Chemical Engineering, Yantai University, Yantai, P.R. China

Received: 30.04.2018 • **Accepted/Published Online:** 17.07.2018 • **Final Version:** 06.12.2018

Abstract: Carbamates weaken the luminol-H_2O_2 chemiluminescence (CL) catalyzed by sodium copper chlorophyll (SCC). The capacity to inhibit the CL of three carbamates is in the order of carbaryl (CBL) >carbofuran (CBF) >metolcarb (MTC). Mechanisms of carbamates inhibiting SCC-luminol-H_2O_2 CL are investigated using fluorescence quenching and quantum chemistry simulations for the first time in this work. Carbamate-SCC interactions studied using fluorescence spectroscopy show that with the increasing concentration of the SCC, the fluorescence of carbamate is quenched regularly, and the quenching mechanism is a static quenching process. Binding constants (K_B) of the three carbamates with SCC are CBL (4.39×10^5) >CBF (1.46×10^4) >MTC (2.16×10^3 L/mol), which is completely harmonious with the capacity to inhibit CL of the carbamates. Furthermore, the carbamate-SCC interaction energies from quantum chemistry simulations are CBL-porphyrin copper (PPCu) (–30.1), CBF-PPCu (–21.0), and MTC-PPCu (–19.9 kJ/mol), which is also identical to their inhibiting capacity. This provides further evidence that the formation of carbamate-SCC complexes reduces the SCC catalytic activity and the CL intensity decreases. In addition, a novel flow injection chemiluminescence method for the determination of carbamate was established based on carbamate inhibiting CL of the SCC-luminol-H_2O_2 CL system under alkaline conditions. This work may contribute to the study of the mechanism of CL inhibition using fluorescence quenching and quantum chemistry calculation methods.

Key words: Chemiluminescence, carbamate-SCC interactions, fluorescence quenching, quantum chemistry calculation

1. Introduction

In recent years, studies of inhibition chemiluminescence (CL) mechanisms have received extensive attention for indirect detection of nonluminescent substances. Some compounds including ligands, metal ions, biologically important antioxidants, and phenolic compounds have been reported to inhibit luminol CL.[1–5] The CL inhibition mechanism may be described as forming a complexation of hydrogen peroxide, suppressing the formation of radicals, or forming a complexation of transition metal catalysts. However, these descriptions are not supported by enough data, because there are no sufficient research means to be used. Therefore, it is very urgent to develop new strategies for studies of the CL inhibition mechanism.

Carbamate is one of the most widely used broad-spectrum pesticides in agriculture and is frequently used as an anesthetic in animal research.[6,7] Carbamate is a well-known carcinogen, and serious health disorders caused by carbamate and its degradation products have been noticed during the last 10 years.[8–12] Recently, we observed that carbamate inhibited luminol-H_2O_2 CL in the presence of sodium copper chlorophyll (SCC).

*Correspondence: zhenboliu@foxmail.com

However, extensive and systematic studies of this inhibited CL were not carried out and the inhibition mechanism was not clear. To understand the inhibition mechanism, it is important to study carbamate in combination with SCC.

There are many research methods for intermolecular interactions. Fluorescence quenching spectra have been used to investigate intermolecular interactions and can give some binding information, such as the binding mechanism, binding modes, binding constants, binding sites, or intermolecular distance.[13−17]. Carbaryl (CBL), carbofuran (CBF), and metolcarb (MTC) (see Figure 1) are three carbamates with fluorescence. In this work, the fluorescence quenching method is used to investigate the carbamate-SCC interaction. On the other hand, quantum chemistry calculations are also used to study the binding of complexation.[12,18,19] All of these research methods are helpful for us to understand the CL inhibition mechanism. To our knowledge, this is the first time the interaction between molecules is studied using fluorescence quenching and quantum chemistry to reveal the CL inhibition mechanism.

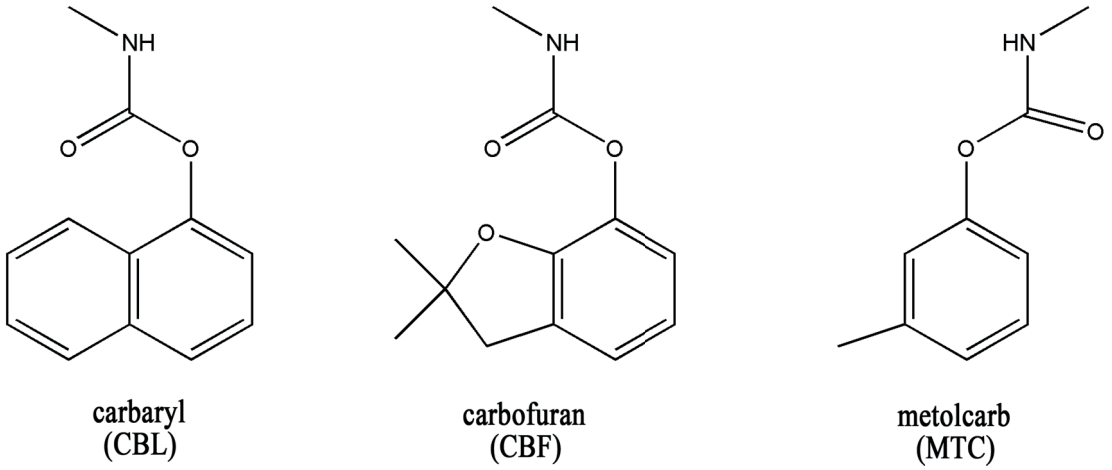

Figure 1. Chemical structures of the three carbamates (CBL, CBF, and MTC).

This paper aims at expounding the regular pattern of inhibition of CL, developing the relationship between inhibited CL and analyte structures, studying fluorescence quenching of carbamate by SCC, investigating the interaction of carbamate with SCC, providing a new idea to investigate the mechanism of CL by fluorescence quenching and quantum chemistry calculation method, and setting up a method to determine three carbamate pesticides (CBL, CBF, and MTC) using CL inhibition methods.

2. Results and discussion

2.1. Static CL of the luminol-H_2O_2 enhanced by SCC

Figure 2 shows the static CL spectra of the SCC-luminol-H_2O_2 system. Comparing curve a and curve b, if there is only luminol with SCC, there is no CL. However, when H_2O_2 is present, strong CL is produced. This means that the CL is produced by the oxidation of luminol by H_2O_2.

For the CL mechanism of the luminol system, previous research works[20] confirmed that the 3-aminophthalate anion is the emitter, and the maximum emission is at 425 nm in the luminol-H_2O_2 system. In this work, the static CL in Figure 2 shows that the maximum peak position of the SCC-enhanced luminol-H_2O_2 CL system is also at 425 nm, which is in agreement with that of the 3-aminophthalate anion.

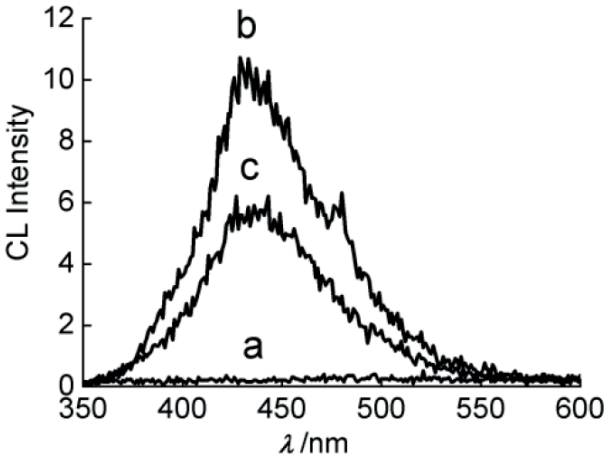

Figure 2. Static CL spectra. $c_{(luminol)}$: 1.0 × 10^{-2} mol/L, $c_{(SCC)}$: 1.0 × 10^{-2} mol/L, H_2O_2(30%), $c_{(carbaryl)}$: 10.0 mg/L. a: SCC-luminol: V($_{luminol}$) : V($_{SCC}$) = 1.50 mL : 1.50 mL. b: SCC-luminol-H_2O_2: V($_{luminol}$) : V($_{SCC}$) : V($_{H2O2}$) = 1.50 mL : 1.50 mL : 0.60 mL. c: CBL-SCC-luminol-H_2O_2: V($_{luminol}$): V($_{SCC}$) : V($_{CBL}$) : V($_{H2O2}$) = 1.50 mL : 1.50 mL : 0.10 µL : 0.60 mL.

2.2. SCC-luminol-H_2O_2 CL inhibited by carbamate

Curves b and c in Figure 2 show that the CL intensity of the SCC-luminol-H_2O_2 system is obviously weakened in the presence of the CBL group. The luminol is oxidized by H_2O_2 in alkaline medium with SCC as a catalyst, while CBL, CBF, and MTC produced great CL inhibition effects. Why and how is the catalytic activity of SCC for CL reaction decreased in the presence of carbamate? The answer may come from further study of the interaction between SCC and carbamate.

2.3. Interaction of SCC with carbamate

The quenching fluorescence spectra of SCC with carbamates (CBL, CBF, and MTC) were measured at 298 and 303 K, as shown in Figure 3. The fluorescence emission spectra show that with the increasing concentration of the SCC, the fluorescences of the three carbamates are all quenched regularly.

According to the literature,[21–23] the fluorescence quenching data were analyzed by the Stern–Volmer equation:

$$\frac{F_0}{F} = 1 + K_{SV}[Q], \tag{1}$$

where F_0 and F are the steady-state fluorescence intensities without and with quencher, respectively; K_{SV} is the Stern–Volmer quenching constant; and [Q] is the concentration of quencher.

The binding constant (K_B) and the numbers of binding sites (n) can be determined by the modified Stern–Volmer equation: [23]

$$\log\frac{F_0 - F}{F} = \log K_B + n\,log\,[Q]. \tag{2}$$

The thermodynamic parameters were evaluated using the following equations:[23]

$$\log K_B = -\frac{H^{\ominus}}{2.303RT} + \frac{S^{\ominus}}{2.303R}, \tag{3}$$

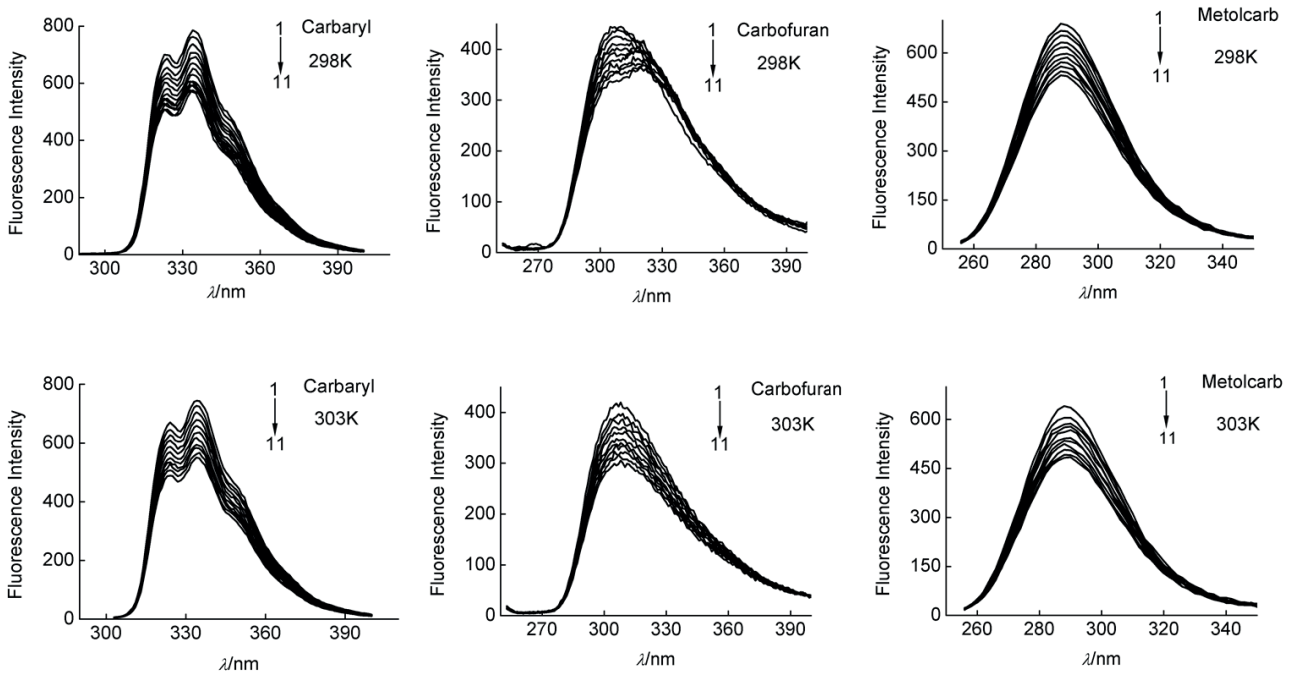

Figure 3. The quenching fluorescence spectra of SCC with CBL, CBF, or MTC at 298 and 303 K. CBL: $\lambda_{ex}/\lambda_{em}$ = 225/335 nm; c_{CBL} =1.0 × 10^{-6} mol/L. CBF: $\lambda_{ex}/\lambda_{em}$ = 225/317 nm; c_{CBF} =1.0 × 10^{-6} mol/L. MTC: $\lambda_{ex}/\lambda_{em}$ = 212/287 nm; c_{MTC} =1.0 × 10^{-6} mol/L. $10^6 c_{scc}$, 1→11: 0.00, 0.67, 1.33, 2.00, 2.67, 3.33, 4.00, 4.67, 5.33, 6.00, 6.67 mol/L.

$$G^{\ominus}=H^{\ominus}-TS^{\ominus}, \tag{4}$$

where R is the gas constant.

According to the above equations, the quenching constant K_{SV}, binding constants K_B, and thermodynamic parameters ($\Delta H^{\ominus}$, $\Delta G^{\ominus}$, $\Delta S^{\ominus}$) between the free and the bound molecules were calculated and are given in Table 1. The K_{SV} values are far greater than 100 L/mol, which indicates that the probable quenching mechanism of fluorescence of carbamate by SCC is a static quenching procedure. The large K_B (K_B >10^4 L/mol) means that there exists a high binding affinity between SCC and carbamates. K_B values of the three carbamates at 303 K follow the order of CBL (4.39 × 10^5) >CBF (1.46 × 10^4) >MTC (2.16 × 10^3 L/mol), which indicates that the CBL group has stronger combining capacity with SCC than CBF and MTC. All the $\Delta G^{\ominus}$ values are negative, showing the spontaneous binding processes. The negative $\Delta S^{\ominus}$ demonstrates that an intermolecular association complex is formed.

2.4. Structure of carbamate-PPCu complexes

Various possible optimized structures of carbamate-PPCu complexes are obtained at the B3LYP/6-31G level (shown in Figure S1 in supporting information). All the single-point energies of the various possible structures are also evaluated at LC-BLYP/6-31+G(d) level, as collected in Table S1, which showed that the most stable structures are CBL-PPCu, CBF-PPCu, and MTC-PPCu (structures presented in Figure 4).

An interesting phenomenon is that the carbonyl groups are close to the Cu atom in PPCu for the stable

Table 1. Quenching constant K_{SV} (L/mol), binding constants K_B (L/mol), and thermodynamic parameters ΔH° (kJ/mol), ΔG° (kJ/mol), and ΔS° (J/mol/K) of carbamate-SCC procedures in different temperatures T (K).

Name	T	K_{SV}	K_B	ΔH°	ΔG°	ΔS°
CBL-SCC	298	5.68×10^4	1.05×10^6	–131	–34.35	–324
	303	5.56×10^4	4.39×10^5	–131	–32.73	–324
CBF-SCC	298	5.03×10^4	5.69×10^5	–550	–32.83	–1736
	303	5.60×10^4	1.46×10^4	–550	–24.15	–1736
MTC-SCC	298	4.44×10^4	3.56×10^4	–421	–25.97	–1325
	303	4.47×10^4	2.16×10^3	–421	–19.34	–1325

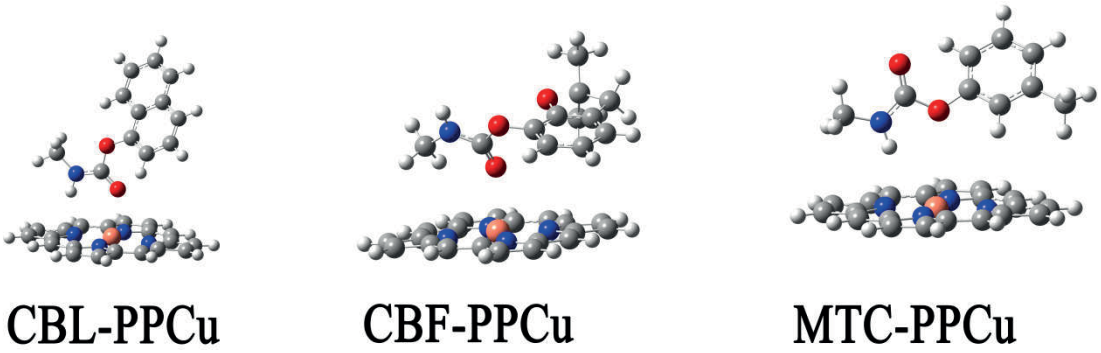

Figure 4. Structures of carbamate-PPCu complexations.

structures of CBL-PPCu and CBF-PPCu, while methylamino is close to the Cu atom for the most stable structure of MTC-PPCu. A comparison of carbamate-PPCu complexes with PPCu (Table 2) indicates that the even distance of Cu-N in the PPCu structure is elongated, and the effect of CBL is largest. The even distance of O-C for the carbonyl group of the carbamate structures is stretched by about 0.01 Å. In addition, NBO charges on PPCu in carbamate-PPCu complexes are all negative, showing the charge shift from carbamate to PPCu. The charges on Cu are changed from 1.015 (PPCu) to 1.005 (CBL-PPCu), 1.013 (CBF-PPCu), and 1.019 (MTC-PPCu), respectively. As can be seen, the carbamate-PPCu interactions partially change structures and charge transfers.

Table 2. The structure parameters (Å), NBO charge (Q, e), and interaction energy (ΔE, kJ/mol).

Name	O-C [a]	Cu-N [b]	Q_{ppCu}	Q_{Cu}	ΔE
CBL-PPCu	1.35	2.04	–0.063	1.005	–30.1
CBF-PPCu	1.35	2.03	–0.058	1.013	–21.0
MTC-PPCu	1.35	2.01	–0.003	1.019	–19.9
CBL	1.36	–	–	–	–
CBF	1.36	–	–	–	–
MTC	1.36	–	–	–	–
PPCu	–	2.01	0	1.015	–

[a] Even distance of O-C for the carbonyl group of the carbamate structures.

[b] Even distance of Cu-N in the PPCu structure.

In the carbamate molecular structure, both the carbonyl oxygen and methylamino can interact with the copper atom in PPCu, but the carbonyl groups have a greater influence on the structures and charges of the PPCu than that of methylamino in the formed carbamate-PPCu complexes. Thus, the binding effect of CBL or CBF with PPCu is stronger than that of MTC. While comparing CBF-PPCu with CBL-PPCu, the space steric hindrance of the two methyl groups in CBF-PPCu may be the reason for the smaller binding effect. The binding strength is in the order of CBL-PPCu >CBF-PPCu >MTC-PPCu.

2.5. Interaction energy

Interaction energies (ΔE) of carbamate-PPCu in Table 2 are –30.1 (CBL-PPCu), –21.0 (CBF-PPCu), and –19.9 kJ/mol (MTC-PPCu), which shows that the stability of the three carbamate-PPCu complexes is in the order of CBL-PPCu >CBF-PPCu >MTC-PPCu. This is consistent with the structure and charge changes of the three carbamate-PPCu complexes discussed in Section 2.4.

In addition, Figure 5 shows that the highest occupied molecular orbital (HOMO) and the lowest unoccupied molecular orbital (LUMO) electronic clouds in carbamate-PPCu are exactly the same as in PPCu. This means that interactions between carbamate and PPCu are not very strong.

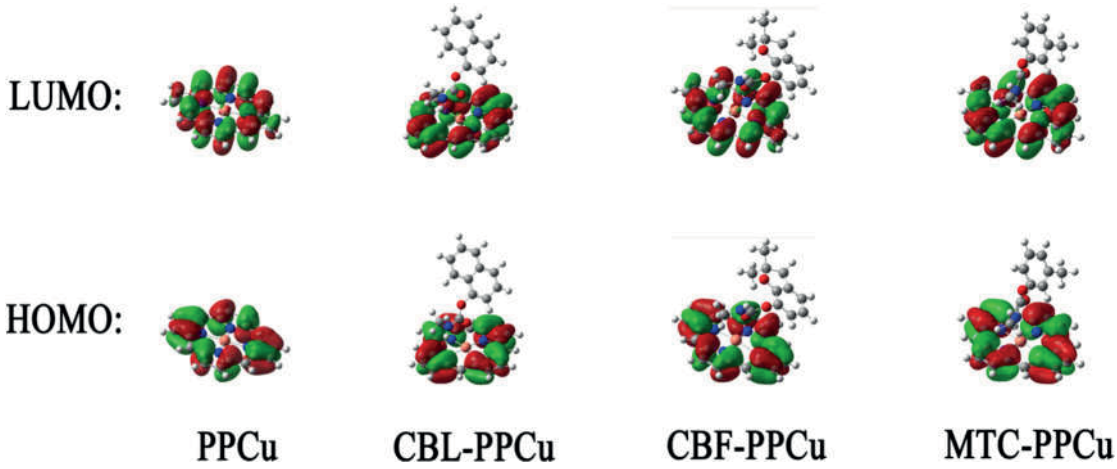

Figure 5. The frontier molecular orbitals of PPCu, CBL-PPCu, CBF-PPCu, and MTC-PPCu. Comparison of their electron densities shows that HOMO and LUMO electronic clouds in carbamate-PPCu are exactly the same as in PPCu.

2.6. Mechanism of inhibited CL

It is obvious that carbamates can inhibit CL signals of the SCC-luminol-H_2O_2 system, and the CL intensity has a linear relationship with the carbamate concentration (see Table 3). In Table 3, the linear equation slope (inhibition sensitivity, S) of the three carbamates becomes greater in the order of 14318 (CBL) >4553 (CBF) >533 mL/μg (MTC), indicating that CBL has the strongest inhibitory effect on this CL system at the same concentration. Furthermore, Figure 6 shows that the K_B and interaction energy ΔE of the three carbamates with SCC are completely consistent with the sensitivity (S) order. Overall, the binding of carbamate to SCC decreases the catalytic activity of SCC for luminol-H_2O_2 CL reaction, as a result of lowered CL intensity. Figure 7 shows the possible mechanism of carbamates reducing the CL intensity enhanced by SCC.

Table 3. The linear equations, inhibition sensitivity S(mL/μg), linear range (μg/mL), and limit of detection LOD (μg/mL).

Name	Linear equations (R^2)	S	Linear range	LOD
CBL	I_{CL} = –14318c+ 11307 (0.9990)	14318	0.03–0.5	0.01
CBF	I_{CL} = –4553c+ 13394 (0.9989)	4553	0.09–1.0	0.03
MTC	I_{CL} = –533c+ 12217 (0.9949)	533	0.50–2.0	0.29

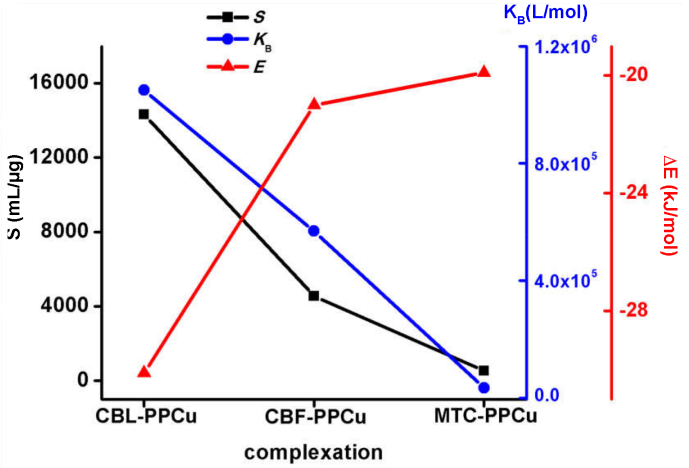

Figure 6. Binding constants (K_B) at 298 K by quenching fluorescence, sensitivity (S) of CL inhibition, and interaction energy (ΔE).

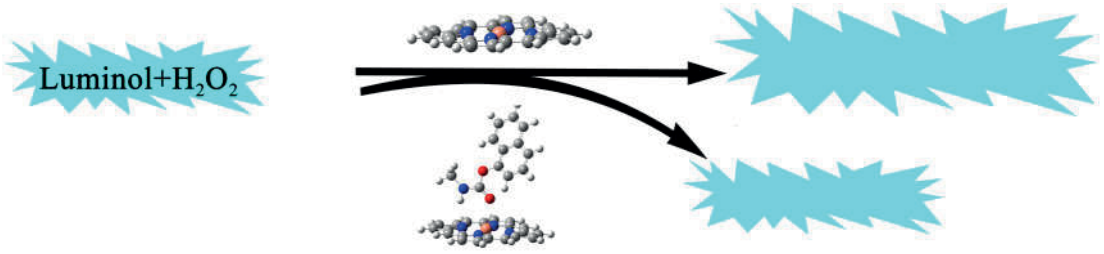

Figure 7. Mechanism of carbamates reducing the CL intensity enhanced by SCC.

2.7. Inhibited CL method for the determination of carbamate

This inhibition in the CL emission is just proportional to the concentration of the carbamate, and a simple and fast new flow injection chemiluminescence (FI-CL) method has been developed for the determination of carbamate. A series of experimental conditions, such as flow rate, pH, and concentrations of luminol, H_2O_2, and SCC, were optimized using a univariate approach for the SCC-luminol-H_2O_2 CL system. The flow rate was studied at the range of 10–40 r/min, the pH at the range of 12.0–13.0, concentrations of luminol at the range of 1.0×10^{-6} to 1.0×10^{-5} mol/L, H_2O_2 at the range of 0.0002–0.005 mol/L, and SCC at the range of 1.0×10^{-6} to 1.5×10^{-5} mol/L. Considering the peak pattern and the signal-to-noise ratio, the optimum obtained conditions were 25 r/min flow rate for the CL system, pH 12.4, 2.0×10^{-6} mol/L for luminol, 0.002 mol/L for H_2O_2, and 1.0×10^{-5} mol/L for SCC.

2.8. Linearity and limit of detection

Under the optimal conditions described above and using the proposed flow injection (FI) manifold, the calibration curve for the determination of CBL, CBF, and MTC is established by injecting each standard analyte solution. Using least squares regression, CL intensity (I_{CL}) is proportional to the carbamate concentration (c) over the studied range with a linear correlation coefficient higher than 0.99 for all the carbamates. The limits of detection (LODs) were calculated (LOD = $3\sigma_{n-1}/S$), and the results are shown in Table 3. In addition to the above, the applied method shows high precision (RSD = 0.5%) with standard deviation (SD) = 50.75 for n = 5 successive injections of blank solution.

2.9. Conclusion

A novel method was developed using an inhibited SCC-luminol-H_2O_2 CL system for highly sensitive detection of carbamate pesticide. Fluorescence quenching and quantum chemistry calculations were used to investigate the mechanism of CL inhibition. The results indicated that carbamate could be bound to SCC, and binding constant K_B values of the three carbamates at 303 K followed the order of CBL (4.39×10^5) >CBF(1.46×10^4) >MTC(2.16×10^3 L/mol). The probable quenching mechanism of the fluorescence of carbamate by SCC is a static quenching procedure. There existed a high binding affinity between SCC and carbamates. Intermolecular association complexes between carbamate and SCC were formed. The interaction between carbamate and PPCu changes the structure and NBO charge. A negative charge transfer from carbamate to PPCu occurred. The order of interaction energy (ΔE) is CBL-PPCu (–30.1) >CBF-PPCu (–21.0) >MTC-PPCu (–19.9 kJ/mol). The orders of K_B and interaction energy ΔE of the three carbamates with SCC were completely harmonious with the inhibition sensitivity (S) order. The catalytic activity of SCC for the CL reaction system decreased and led to the lowered CL intensity.

3. Experimental

3.1. Instrumentation

CL measurements were made by means of a model MPI-B-IFIS-C analysis system (Xi'an Remex Electronic Science-tech, China). The excitation and emission spectra were measured on a Varian Cary-ELIPSE fluorescence spectrophotometer (Varian, USA).

3.2. Reagents

Analytical reagent chemicals were used without further purification. High-purity water was used for the preparation of solutions. Luminol ($C_8H_7N_3O_2$, purity >98%, Alfa Aesar, USA) stock solution (0.01 mol/L) was prepared by dissolving 0.4430 g in 0.1 mol/L sodium hydroxide and diluting 250 mL, and it was stored for at least 3 days in a refrigerator to attain stability before use. Sodium copper chlorophyll (SCC, Yantai Libo Pharmaceutical Company, China) stock solution (1.0×10^{-3} mol/L) was prepared by dissolving 0.1850 g in water and diluting 250 mL. The stock solutions were further diluted as working solutions prior to use. Working solutions of H_2O_2 were prepared fresh daily from 30% (v/v) H_2O_2 (Suzhou Crystal Clear Chemical Company, China). The buffer solution was adjusted to pH 12.0–13.0 with 0.2 mol/L KCl and 0.2 mol/L NaOH. CBL, CBF, and MTC (purity >98.5%, Ehrenstorfer GmbH, Germany) stock solution (1.0×10^{-4} mol/L) was prepared by dissolving the standard in ethanol and stored at 0–4 °C.

3.3. Computational details

PPCu, the center structure of SCC, plays a major role as the catalyst of the CL process in this research. In order to simplify our study, PPCu was used as a template to simulate the interaction of SCC with carbamate. Optimized structures of carbamate-PPCu with all real frequencies were obtained at the B3LYP/6-31G level. Interaction energies (ΔE) were calculated as the difference between the energy of the complex and the energy sum of the isolated monomers, and were corrected for the basis set superposition error (BSSE) by the standard counterpoise method of Boys and Bernardi.[24] Interaction energies were evaluated using long-range corrected functional LC-BLYP with the 6-31+G(d) basis set in this work. NBO analyses were carried out at the LC-BLYP/6-31+G(d) level with NBO version 3.1 implemented in GAUSSIAN 09 to reveal the bonding nature in view of charge transfer and orbital interactions. All calculations were performed using the GAUSSIAN 09 package.[25]

3.4. Experimental method of static CL

In order to investigate effects of SCC and carbamate, static CL responses were researched using a fluorescence spectrophotometer. SCC, SCC-H_2O_2, and CBL-SCC-H_2O_2 solutions were respectively injected into a detection cell that contained alkaline luminol solution. The static CLs of the SCC-luminol-H_2O_2 system were detected in the wavelength range of 350–600 nm by fluorescence spectrophotometer.

3.5. Experimental method of CL

As shown in Figure 8, the FI configuration consisted of a three-channel manifold where either standards or sample solutions were incorporated into a H_2O_2 solution carrier with the aid of a manual injection valve. Prior to the CL measurement acquisition corresponding to solutions containing SCC, the alkaline luminol solution stream was mixed with the carbamate sample or blank solution stream in a three-way T connector. The resulting stream was then mixed with the H_2O_2 carrier solution into the detection cell and the CL emission resulting from the oxidation of luminol without carbamate was recorded as the background blank signal. Then the inhibition CL signal of the system was detected in the presence of carbamate.

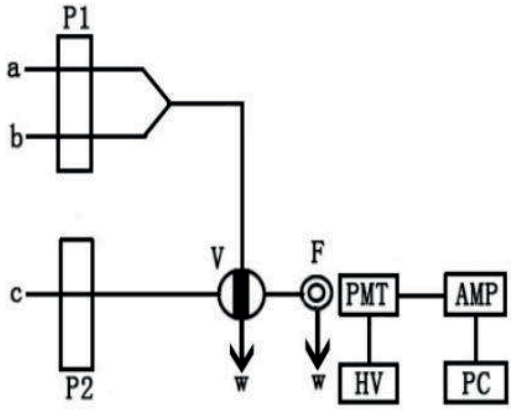

Figure 8. Schematic diagram of the flow injection chemiluminescence system. a: Luminol + SCC; b: sample or blank solution; c: H_2O_2; P: Pump; V, injector; F, flow cell; AMP, amplifier; w, waste; HV, high voltage; PMT, photomultiplier tube; PC, computer.

3.6. Fluorescence quenching spectra

Carbamates (CBL, CBF, and MTC) were dissolved in alcohol, the final concentration of carbamates was 1.0×10^{-6} mol/L, and 3.0 mL of carbamate solution was transferred to a 1.0-cm quartz cell. Then the SCC stock solutions were gradually titrated into the cell using a microinjector, and the accumulated volumes were smaller than 100 µL to avoid unnecessary volume increment. Under the apparatus conditions of both entrance slit and exit slit width at 10 nm and scanning speed at 60 nm/min, fluorescence quenching spectra were obtained in the range of 250–450 nm with $\lambda_{ex}/\lambda_{em}$ = 225/335 nm for CBL, $\lambda_{ex}/\lambda_{em}$ = 225/317 nm for CBF, and 212/287 nm for MTC.

Acknowledgment

The authors express their thanks to the Natural Science Foundation of Shandong Province for its financial support under project number ZR2013BM016 and ZR2016BM23, and the Special Foundation of Youth Academic Backbone of Yantai University.

References

1. Cui, H.; Meng, R.; Jiang, H.; Sun, Y.; Lin, X. *Luminescence* **1999**, *14*, 175-182.
2. Whitehead, T. P.; Thorpe, G. H. G.; Maxwell, S. R. J. *Anal. Chim. Acta* **1992**, *266*, 265-277.
3. MacDonald, A.; Nieman, T. A. *Anal. Chem.* **1985**, *57*, 936-940.
4. Koerner, P. J.; Nieman, T. A. *Microchim. Acta* **1987**, *92*, 79-90.
5. Han, S.; Liu, E.; Li, H. *Luminescence* **2006**, *21*, 106-111.
6. Petropoulou, S. S. E.; Gikas, E.; Tsarbopoulos, A.; Siskos, P. A. *J. Chromatogr. A* **2006**, *1108*, 99-110.
7. Aprea, C.; Colosio, C.; Mammone, T.; Minoia, C.; Maroni, M. *J. Chromatogr. B* **2002**, *769*, 191-219.
8. Forman, S.; Novák, J.; Tykva, R.; Kás, J.; Wimmer, Z.; Ruml, T. *Chemosphere* **2002**, *46*, 209-217.
9. Fernández, J. M.; Vázquez, P. P.; Vidal, J. L. M. *Anal. Chim. Acta* **2000**, *412*, 131-139.
10. Bolognesi, C. *Mutat. Res.* **2003**, *543*, 251-272.
11. Knaak, J. B.; Yee, K.; Ackerman, C. R.; Zweig, G.; Fry, D. M.; Wilson, B. W. *Toxicol. Appl. Pharmacol.* **1984**, *76*, 252-263.
12. López-Paz, J. L.; Catalá-Icardo, M. *Anal. Lett.* **2011**, *44*, 146-175.
13. Bordbar, A. K.; Taheri-Kafrani, A. *Colloid. Surface. B* **2007**, *55*, 84-89.
14. Cui, F.; Zhang, Q.; Yao, X.; Luo, H.; Yang, Y.; Qin, L.; Qu, G.; Lu, Y. *Pestic. Biochem. Physiol.* **2008**, *90*, 126-134.
15. Cui, F.; Qin, L.; Zhang, G.; Liu, Q.; Yao, X.; Lei, B. *J. Pharm. Biomed. Anal.* **2008**, *48*, 1029-1036.
16. Hu, Y. J.; Liu, Y.; Pi, Z. B.; Qu, S. S. *Bioorg. Med. Chem.* **2005**, *13*, 6609-6614.
17. van de Weert, M.; Stella, L. *J. Mol. Struct.* **2011**, *998*, 144-150.
18. Zierkiewicz, W.; Fanfrlík, J.; Hobza, P.; Michalska, D.; Zeegers-Huyskens, T. *Theor. Chem. Acc.* **2016**, *135*, 1-11.
19. Wei, Q.; Li, Q.; Cheng, J.; Li, W.; Li, H.-B. *RSC Adv.* **2016**, *6*, 79245-79253.
20. Paul, D. B. *Talanta* **1978**, *25*, 377-382.
21. Feng, X. Z.; Lin, Z.; Yang, L. J.; Wang, C.; Bai, C. L. *Talanta* **1998**, *47*, 1223-1229.
22. Kandagal, P. B.; Ashoka, S.; Seetharamappa, J.; Shaikh, S. M. T.; Jadegoud, Y.; Ijare, O. B. *J. Pharm. Biomed. Anal.* **2006**, *41*, 393-399.
23. Guo, Y.; Yue, Q.; Gao, B. *Environ. Toxicol. Pharmacol.* **2010**, *30*, 45-51.

24. Boys, S. F.; Bernardi, F. *Mol. Phys.* **1970**, *19*, 553-566.

25. Frisch, M. J.; Trucks, G. W.; Schlegel, H. B.; Scuseria, G. E.; Robb, M. A.; Cheeseman, J. R.; Scalmani, G.; Barone, V.; Mennucci, B.; Petersson, G. A. et al. *Gaussian 09, Revision. A.02*; Gaussian, Inc.: Wallingford, CT, USA, 2009.

Supporting Information

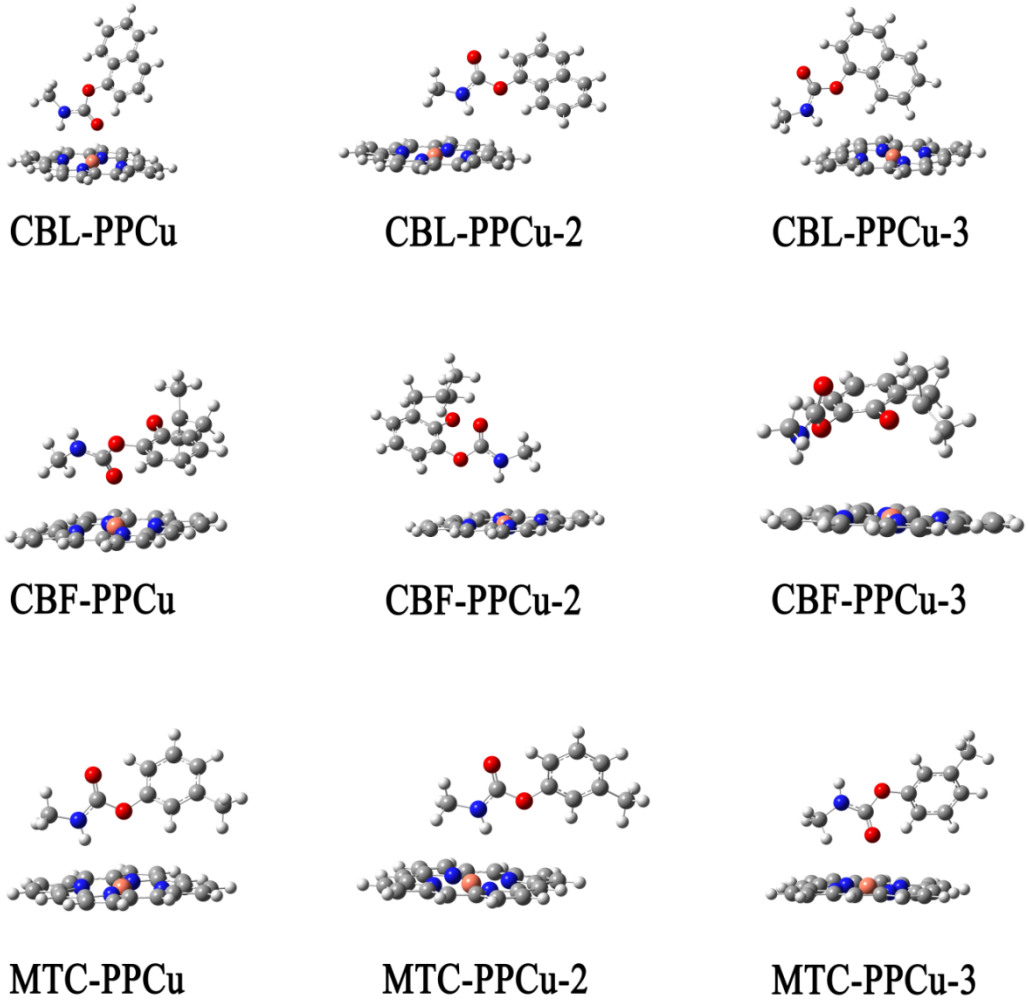

Figure S1. Various possible structures of carbamate-PPCu optimized at LC-BLYP/6-31 + G(d) level.

Table S1. Single-point energy values of carbamate-PPCu structures.

Structure	Single energy (a.u.)
CBL-PPCu	–3297.4379
CBL-PPCu-2	–3297.4375
CBL-PPCu-3	–3297.4366
CBF-PPCu	–3375.0297
CBF-PPCu-2	–3375.0295
CBF-PPCu-3	–3375.0285
MTC-PPCu	–3183.1380
MTC-PPCu-2	–3183.1373
MTC-PPCu-3	–3183.1369